J. CHEM. SOC. FARADAY TRANS., 1992, 88(17), 2437–2444

2-Bromoethylperoxy and 2-Bromo-1-methylpropylperoxy Radicals: Ultraviolet Absorption Spectra and Self-reaction Rate Constants at 298 K

John N. Crowley* and Geert K. Moortgat
Max-Planck-Institut für Chemie (Division of Atmospheric Chemistry), Saarstrasse 23, 6500 Mainz, Germany

The self-reaction rate constants and UV absorption spectra of two brominated peroxy radicals, $BrCH_2CH_2O_2$ (2-bromoethylperoxy) and $(CH_3)BrCHCH(CH_3)O_2$ (2-bromo-1-methylpropylperoxy) have been measured using the molecular modulation technique. Self-reaction rate constants (k_{obs}) of $(6.2 \pm 1.2) \times 10^{-12}$ and $(9.6 \pm 1.9) \times 10^{-13}$ cm^3 $molecule^{-1}$ s^{-1} were obtained for $BrCH_2CH_2O_2$ and $(CH_3)BrCHCH(CH_3)O_2$, respectively. In both cases secondary chemistry is likely to enhance the removal rate of the radicals and the given rate constants are expected to be slightly higher than the true value. The UV spectra of both radicals are broad absorptions with maxima close to 240 nm. Absolute cross-sections at 270 nm were found to be $(2.2 \pm 0.4) \times 10^{-18}$ and $(2.8 \pm 0.6) \times 10^{-18}$ cm^2 $molecule^{-1}$ for $BrCH_2CH_2O_2$ and $(CH_3)BrCHCH(CH_3)O_2$, respectively. The measured values of self-reaction rate constants and UV absorption spectra are compared to results for $C_2H_5O_2$. In addition, a long-lived transient absorption was observed in the $BrCH_2CH_2O_2$ experiments, and is thought to be due to $BrCH_2CH_2OOBr$, a product of an association reaction between Br atoms and $BrCH_2CH_2O_2$.

Recognition of the important role of peroxy radical reactions in the atmospheric degradation of hydrocarbons has resulted in extensive efforts toward understanding the factors which control the reactivities of peroxy radicals towards each other.[1]

As described in a recent review of organic peroxy radical kinetics,[1] the rate constants for simple alkylperoxy-radical self-reactions are known to vary greatly with length of carbon chain and the degree and position of substitution of H atoms by either CH_3 or OH groups or halogen atoms. For example, the self-reaction rate constant for $ClCH_2CH_2O_2$ (2-chloroethylperoxy) is enhanced by a factor *ca.* 30 over the unsubstituted ethylperoxy radical ($C_2H_5O_2$).[2] To date, studies of several chlorinated and fluorinated analogues of methyl- and ethyl-peroxy radicals have been made, but the data on brominated peroxy radicals covers the bromomethylperoxy radical ($BrCH_2O_2$) only.[3] In this work we extend the database on brominated peroxy radicals by examining, *via* the molecular modulation technique, the self-reaction rate constants of 2-bromoethylperoxy and 2-bromo-1-methylpropylperoxy radicals.

Experimental

The molecular modulation apparatus has recently been described[4] and only those details directly relevant to the present measurements are recounted here. All experiments were carried out in a temperature-stabilised (298 ± 2 K) cylindrical quartz reaction vessel with internal White optics. Absorption of light from a deuterium lamp over a 9.75 m pathlength was monitored by either a photomultiplier tube–monochromator arrangement at a single wavelength (resolution *ca.* 1.5 nm) or by a diode-array camera (resolution better than 0.2 nm). Modulated production of the peroxy radicals was achieved by the regularly interrupted photolysis of flowing gas mixtures containing suitable precursors. Gas flows and photolysis duty-cycles were chosen so that product build-up was avoided. As photolysis source, 6 Philips TL03 lamps provided a homogeneous light flux (380 to 470 nm) over the entire length of the cell. In order to prevent light from the photolysis lamps entering the monochromator, a 10 cm long quartz cell filled with *ca.* 17 Torr† Br_2 was placed directly before the entrance slit.

The peroxy radicals were produced by the addition of a Br atom to the double bond of either ethene (C_2H_4) or (*E*)-but-2-ene (C_4H_8) in the presence of O_2. The TL03 lamps emit strongly between 380 and 470 nm and provide an efficient means of Br atom production from molecular Br_2. Both Br ($^2P_{3/2}$) and spin–orbit-excited Br ($^2P_{1/2}$) are produced at these wavelengths,[5] but Br ($^2P_{1/2}$) is quenched rapidly by O_2 and N_2 ($k_2 = 3.4 \times 10^{-11}$ and 2.5×10^{-15} cm^{-3} $molecule^{-1}$ s^{-1} for O_2 and N_2, respectively) and is not expected to react with the alkene.

$$Br_2 + h\nu\ (380\text{–}470\ nm) \rightarrow Br\ (^2P_{1/2}) + Br\ (^2P_{3/2}) \quad (1)$$

$$Br\ (^2P_{1/2}) + N_2/O_2 \rightarrow Br\ (^2P_{3/2}) + N_2/O_2 \quad (2)$$

$$Br\ (^2P_{3/2}) + C_2H_4 + M \rightarrow BrCH_2CH_2 + M \quad (3)$$

$$BrCH_2CH_2 + O_2 + M \rightarrow BrCH_2CH_2O_2 + M \quad (4)$$

$$Br\ (^2P_{3/2}) + C_4H_8 + M \rightarrow (CH_3)BrCHCH(CH_3) + M \quad (5)$$

$$(CH_3)BrCHCH(CH_3) + O_2 + M \rightarrow (CH_3)BrCHCH(CH_3)O_2 + M \quad (6)$$

The peroxy radicals will then undergo self-reaction:

$$2\ BrCH_2CH_2O_2 \rightarrow products \quad (7)$$

$$2\ (CH_3)BrCHCH(CH_3)O_2 \rightarrow products \quad (8)$$

The chosen modulation cycle was 4 s in the $BrCH_2CH_2O_2$ experiments and 10 s for $(CH_3)BrCHCH(CH_3)O_2$. In both cases a 10% lights-on duty-cycle was used and modulated absorption profiles were gathered during the first 50% of each cycle.

Flows of high-purity C_2H_4, C_4H_8, O_2 and N_2 were directed into the reaction vessel through calibrated flow-controllers. Gas-phase Br_2 was introduced quantitatively into the cell by passing a flow of N_2 over a sample of Br_2 (liquid) held at 0 °C, and measuring its concentration by optical absorption at 420 nm both before and after each experiment.

† 1 Torr = (101 325/760) Pa.

The concentrations of all other gases were calculated from their partial flows and the total pressure in the cell. Typical gas flows were *ca.* 4–5 dm^3 min^{-1}, giving residence times in the cell of *ca.* 10, 20 and 30 s at 200, 400 and 600 Torr, respectively.

The peroxy radicals produced in reactions (4) and (6) were followed directly by their time-resolved UV absorption at a single wavelength (usually 270 nm) to extract both UV cross-sections and kinetic data for the self-reaction. Relative absorptions (at 10 nm intervals between 200 and 290 nm) were measured to give the UV absorption spectrum of each radical. All experiments were carried out at 298 ± 2 K, and at total pressures of 200, 400 and 600 Torr. The effect of varying the partial pressures of C_2H_4 and O_2 was also investigated.

Results

Analysis of Modulated Waveforms

The analysis of modulated absorptions to give kinetic and cross-section data has been described in detail by Jenkin and Cox.[7] At its steady-state concentration, the absorbance (A) due to a peroxy radical following second-order kinetics is given by:

$$(A)_{ss}^2 = (\sigma_\lambda^2/k_{obs})Bl^2 \quad \text{(I)}$$

where B is the radical production rate, l the optical path length, σ_λ the absorption cross-section at wavelength λ, and k_{obs} is the observed second-order decay rate. The gradient of a plot of inverse absorbance during the dark phase of the modulation cycle ($B = 0$) *vs.* time is equal to $2k_{obs}/\sigma_\lambda l$:

$$1/A_t = 1/A_{t=0} + 2k_{obs}t/\sigma_\lambda l \quad \text{(II)}$$

The measurement of B, which is equal to $k_{phot}[Br_2]$, where k_{phot} is the photolysis constant for Br_2, thus enables both k_{obs} and σ_λ to be extracted from eqn. (I) and (II).

In neither $BrCH_2CH_2O_2$ nor $(CH_3)BrCHCH(CH_3)O_2$ experiments was a true steady-state absorption observed (where $dA/dt = 0$), instead a linear increase in absorption during the latter part of the photolysis period. This indicates formation of a product which absorbs at 270 nm and which, over a 1 s timescale, behaves like a stable molecule. The rate of formation of a stable species (product) in a flowing system is approximated during the lights-on period by:

$$d[product]/dt = k_{obs}[RO_2]^2 - k_f[product] \quad \text{(III)}$$

where k_f is the rate constant for flow out of the cell. This has the effect of superimposing a near triangular function on the modulated waveform.[8] In order to extract the steady-state absorption due only to the radical, A_{ss}, a linear function with a gradient equal to the measured dA/dt is subtracted from the lights-on part of the modulated profile. Absorption by the product also perturbs the decay trace away from pure second-order kinetics. For this reasons the decays were fitted to an algorithm of the form shown below:

$$f(t) = A_1/(t + c) + A_2 + A_3 t \quad \text{(IV)}$$

where A_1 is the second-order decay term, A_2 allows for the non-zero concentration of $BrCH_2CH_2O_2$ or $(CH_3)BrCHCH(CH_3)O_2$ before the next modulated cycle begins and A_3 represents the approximately linear part of the decay due to stable product flow out. This is referred to in the text as a modified second-order analysis and its validity is examined in detail in the discussion.

Photolysis Constant of Br_2

The value of B was measured by observing the first-order decay of Br_2 during the photolysis of static Br_2–C_2H_4–O_2–N_2 mixtures at either 400 or 600 Torr total pressure. In all experiments the decay of Br_2 was monitored at 500 nm where there is no absorption by any of the expected products. Variation of the C_2H_4 partial pressure between 7 and 20 Torr and the O_2 partial pressure between 80 and 400 Torr resulted in no significant change in the measured first-order decay rate. The photolysis constant, k_{phot}, which was measured on several occasions during the course of the experiments, was found to be either $(1.54 \pm 0.02) \times 10^{-2}$ or $(1.65 \pm 0.02) \times 10^{-2}$ s^{-1}. No obvious reason was found for the fluctuation of k_{phot} between these two values and it was necessary to carry out photolysis-constant measurements at regular intervals to determine which value should be used in evaluating the kinetic data.

Owing to the relatively high photolysis constant, k_{phot}, and long residence times at 400 or 600 Torr, the initial Br_2 concentration $[Br_2]_0$ was not equal to that after 20 modulation cycles when the system was in equlibrium, *i.e.* $[Br_2]_{eq}$. Data were therefore collected only after the first 20 or so cycles were complete and the Br_2 oscillated about an equilibrium value determined by the ratio of the lights-on to lights-off periods, its residence time in the cell and its initial concentration. Numerical simulations were carried out to calculate $[Br_2]_{eq}$ for a given experiment. For 200 Torr experiments this resulted in a downwards correction of $[Br_2]_0$ by *ca.* 2%, increasing to *ca.* 4% and 6% for 400 and 600 Torr, respectively. The corrected values of $[Br_2]_{eq}$ were used in the kinetic analysis.

$BrCH_2CH_2O_2$

Two typical modulated waveforms at 270 nm, obtained in the photolysis of flowing Br_2–C_2H_4–O_2–N_2 mixtures at total pressures of 200 and 600 Torr are displayed in Fig. 1. As discussed above, these waveforms reveal a linear increase in absorption during the latter phase of the photolysis period, and the rate of increase carries information about the rate of production of the absorbing stable molecule during the radical steady-state phase. In these experiments the rate of production of the stable absorber, $(dA/dt)_{ss}$, was seen to be dependent on the partial pressures of both C_2H_4 and O_2, with low partial pressures of both resulting in more rapid product formation. This is illustrated in Table 1 where the C_2H_4 and Br_2 partial pressures are listed along with $(dA/dt)_{ss}$, and in Fig. 1 which represents the two extreme

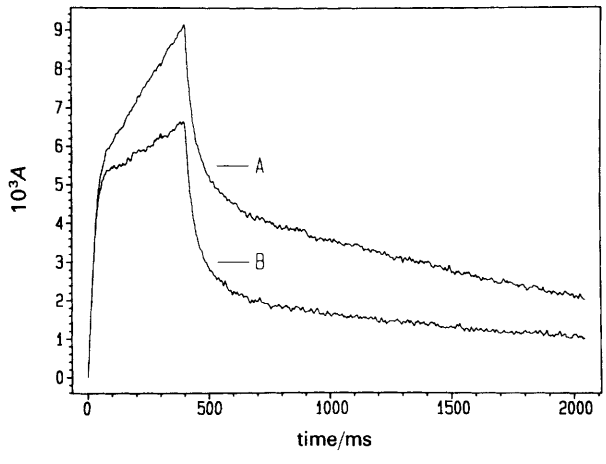

Fig. 1 Modulated absorption profiles due to $BrCH_2CH_2O_2$ and stable product(s) at 270 nm in the Br_2–C_2H_4–O_2–N_2 system. A, 80 Torr O_2, 7 Torr C_2H_4, total pressure 200 Torr. B, 240 Torr O_2, 10 Torr C_2H_4, total pressure 600 Torr. $[Br_2]$ *ca.* 1.5×10^{15} molecule cm^{-3} in both cases

Table 1 Kinetic and UV cross-section data for $BrCH_2CH_2O_2$ at 270 nm

expt.	pressure /Torr	$[Br_2]_{eq}$ /10^{15} molecule cm^{-3}	$[C_2H_4]$ /Torr	$[O_2]$ /Torr	$(dA/dt)_{ss}$ /10^{-6} s^{-1}	σ_{270} /10^{-18} cm^2 molecule^{-1}	k_{7obs} /10^{-12} cm^3 molecule^{-1} s^{-1}
1	200	2.21	7	78	9.86	2.38	6.67
2	200	1.73	7	78	7.72	2.22	6.50
3	200	1.92	7	188	5.85	2.17	7.01
4	200	1.97	7	83	7.34	2.40	7.30
5	200	2.06	7	188	5.82	2.32	6.98
6	200	1.85	13	75	6.29	2.26	6.86
7	200	1.95	2	80	12.9		
8	400	1.94	7	158	5.60	2.26	6.35
9	400	1.83	7	83	4.44	2.21	6.17
10	400	1.82	14	254	3.37	2.09	5.94
11	400	1.56	12	138	3.44	2.18	6.13
12	400	1.55	12	138	3.38	2.24	6.14
13	400	1.55	12	138	3.44	2.18	6.34
14	400	1.75	12	138	4.34	2.20	5.95
15	400	1.71	17	136	3.39	2.22	5.84
16	400	1.73	17	136	3.84	2.00	5.33
17	400	1.74	17	136	3.52	2.14	5.89
18	400	1.67	17	136	3.33	2.27	6.24
19	400	1.57	17	136	2.67	2.29	6.55
20	600	1.76	17	202	2.98	2.22	6.02
21	600	2.08	10	237	4.16	2.35	6.82
22	600	1.52	17	202	2.78	2.22	6.24
23	600	1.55	17	202	2.47	2.06	5.75
24	600	1.51	17	202	2.24	2.41	6.95

cases. This behaviour was unexpected and led us to carry out investigations of the nature of the absorbing products.

UV Product Studies

The stable products of $BrCH_2CH_2O_2$ self-reaction have been shown to be $BrCH_2CH_2OH$, $BrCH_2CHO$, H_2O_2 and $BrCH_2CH_2OOH$,[9] which arise as a result of the following reactions:

$$2\ BrCH_2CH_2O_2 \rightarrow 2\ BrCH_2CH_2O + O_2 \quad (7a)$$

$$\rightarrow BrCH_2CHO + BrCH_2CH_2OH + O_2 \quad (7b)$$

$$BrCH_2CH_2O + O_2 \rightarrow BrCH_2CHO + HO_2 \quad (9)$$

$$BrCH_2CH_2O_2 + HO_2 \rightarrow BrCH_2CH_2OOH + O_2 \quad (10)$$

$$2\ HO_2 \rightarrow H_2O_2 + O_2 \quad (11)$$

Experiments were carried out to test for C_2H_4 or O_2 pressure dependence on the formation of products. Two static experiments were carried out, one with low C_2H_4 and low O_2 partial pressures (at 200 Torr), and the second with high C_2H_4 and O_2 partial pressures (at 600 Torr), similar to the conditions outlined in Fig. 1. In this case static mixtures were irradiated for 30 s and the contents of the cell then examined for products by diode-array UV spectroscopy. The spectra reveal the presence of an absorption between *ca.* 250 and 350 nm which shows the typical structure of an aldehyde, but shifted *ca.* 20 nm to longer wavelength as compared with acetaldehyde. This absorption is presumably due to $BrCH_2CHO$. The UV absorption spectrum of $BrCH_2CH_2OH$ was measured in separate experiments and found to be similar in shape and position to a second, stronger absorption at shorter wavelengths. This absorption can therefore be assigned, at least in part, to $BrCH_2CH_2OH$, with some contribution from H_2O_2 and especially $BrCH_2CH_2OOH$ also expected.

The most important result from the static experiments is that the absorption due to stable species outlined above is not dependent on the O_2 or C_2H_4 partial pressures, as both experiments gave identical results. This should be compared with the modulated absorption profiles at 270 nm where the slopes during the latter part of the photolysis period, $(dA/dt)_{ss}$, are 9.9×10^{-6} and 4.2×10^{-6} s^{-1} at 200 and 600 Torr, respectively, more than a factor of two different. This suggests that the species responsible for the increasing absorption during the lights-on period in the modulated photolysis experiments is not one of the expected stable products, but one that is no longer present *ca.* 20 s after photolysis has ceased. The fact that the increase in absorption is linear over a 0.4 s timescale indicates that we are dealing with a semi-stable molecule. A possible candidate is $BrCH_2CH_2OOBr$, formed in an association reaction between Br and $BrCH_2CH_2O_2$:

$$Br + BrCH_2CH_2O_2 + M \rightarrow BrCH_2CH_2OOBr + M \quad (12)$$

The dependence of the rate of formation of $BrCH_2CH_2OOBr$ on both $[O_2]$ and $[C_2H_4]$ is explained by invoking an equilibrium between Br atoms, C_2H_4 and BrC_2H_4:

$$Br + C_2H_4 + M \rightleftharpoons BrC_2H_4 + M \quad (3, -3)$$

$$BrC_2H_4 + O_2 + M \rightarrow BrC_2H_4O_2 + M \quad (4)$$

$$BrC_2H_4O_2 + Br + M \rightleftharpoons BrC_2H_4OOBr + M \quad (12, -12)$$

The rate of BrC_2H_4OOBr production is dependent on the concentrations of both C_2H_4 and O_2 if reaction (3) is an equilibrium as outlined. Further evidence for this equilibrium is provided by Barnes *et al.*,[10] who interpreted an O_2 partial pressure dependence for the reaction between Br and C_2H_4 in terms of reactions (3) and (-3). The fate of BrC_2H_4OOBr may be to decompose to $BrC_2H_4O_2 + Br$ [reaction (-12)] or it may react with Br atoms:

$$Br + BrC_2H_4OOBr \rightarrow BrC_2H_4O_2 + Br_2 \quad (13)$$

In either case, if BrC_2H_4OOBr is present during the latter phase of the photolysis period it should be possible to measure its UV spectrum. Experiments were therefore carried out using time-resolved diode-array spectroscopy, which has been utilised before in this laboratory to measure the UV spectra of radicals such as HO_2[11] and $C_2H_5O_2$.[4] In these

experiments, the diode-array camera is triggered to measure absorption at predetermined time intervals in the modulation cycle. For the purpose of these experiments, only the spectra obtained during the latter stage of the lights-on period were analysed, as these are expected to contain the highest concentrations of BrC_2H_4OOBr. Two experiments were carried out, one with low C_2H_4 and O_2 partial pressures to favour BrC_2H_4OOBr production (exp. A), and one with high C_2H_4 and O_2 to prevent its production (exp. B). The two spectra thus obtained both contain stable product absorption as expected. Upon subtracting the spectrum in exp. B from that in exp. A, the resultant spectrum of the proposed transient BrC_2H_4OOBr was obtained. This is shown in Fig. 2 which reveals a broad unstructured absorption between 230 and 310 nm with a maximum at *ca.* 260 nm, although a slight shift in λ_{max} due to the presence of unequal amounts of $BrCH_2CH_2O_2$ in exp. A and B cannot be ruled out.

In order to help confirm the assignment of the transient absorption to BrC_2H_4OOBr, experiments were carried out in which Br atoms were produced in the presence of ethylperoxy radicals ($C_2H_5O_2$) with the aim of producing C_2H_5OOBr. This species might be expected to show a similar absorption spectrum and transient behaviour to BrC_2H_4OOBr. The modulated photolysis of Cl_2–C_2H_6–O_2–N_2–Br_2 mixtures was the source of both $C_2H_5O_2$ and Br.

$$Cl_2 + h\nu\ (275\text{–}365\ nm) \rightarrow Cl + Cl \quad (14)$$

$$Cl + C_2H_6 \rightarrow C_2H_5 + HCl \quad (15)$$

$$C_2H_5 + O_2 + M \rightarrow C_2H_5O_2^{\cdot} + M \quad (16)$$

Careful choice of conditions ensured that Cl atoms were converted stoichiometrically to $C_2H_5O_2$ as previously reported.[4] Given the slow self-reaction rate constant of $C_2H_5O_2$ (*ca.* 1×10^{-13} cm^3 molecule^{-1} s^{-1}), the concentration of [Cl_2] (*ca.* 5×10^{15} molecule cm^{-3}) and photolysis constant for Cl_2, (2×10^{-3} s^{-1}) a steady-state $C_2H_5O_2$ concentration of *ca.* 1×10^{13} molecule cm^{-3} is expected. Br_2 is photolysed inefficiently by TL12 lamps, but as their only likely reactive partner in this system is $C_2H_5O_2$, nearly all Br atoms should be scavenged to make C_2H_5OOBr if this reaction proceeds rapidly under our experimental conditions.

$$C_2H_5O_2 + Br + M \rightarrow C_2H_5OOBr + M \quad (17)$$

Time-resolved diode-array experiments were carried out with spectra gathered at 0.4 s time intervals both during and after the lights-on period of the modulation cycle. Fig. 3 shows absorption measurements made at 1.2, 1.6, 2.0 s *etc.* after the photolysis period was complete. Spectra measured during the photolysis period suffered from interference from $C_2H_5O_2$ absorption and are not presented.

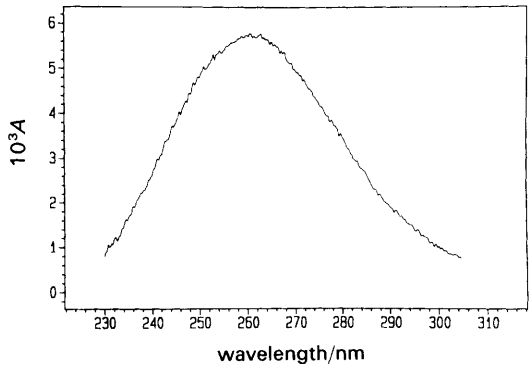

Fig. 2 Absorption spectrum of the transient BrC_2H_4OOBr molecule obtained by triggered diode-array absorption spectroscopy. The spectrum was obtained during the lights-on phase of a modulation cycle in a flowing experiment at 200 Torr (concentrations of [Br_2], C_2H_4 and O_2 as in Fig. 1, B)

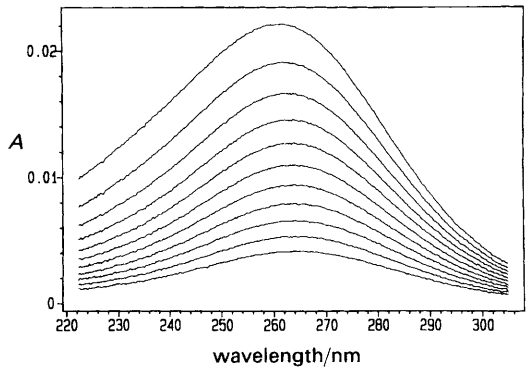

Fig. 3 Time-resolved absorption spectrum of C_2H_5OOBr formed in the Cl_2–C_2H_6–O_2–Br_2 system. The uppermost absorption was measured 1.2 s after the photolysis lights were turned out, with subsequent measurements at 0.4 s intervals

Fig. 3 reveals a transient absorption which, similar to that seen in the Br_2–C_2H_4–O_2–N_2 system, is broad and unstructured with a λ_{max} at *ca.* 264 nm. At shorter times the maximum appears to be shifted to shorter wavelengths, presumably due to a contribution to the absorption by $C_2H_5O_2$ which has a λ_{max} at *ca.* 240 nm and decays more rapidly than the transient absorber. The transient absorption has almost disappeared *ca.* 5 s after the photolysis has ceased, and would therefore not be detected in the experiments designed to detect stable products.

This observation is further evidence that the transient absorber is an ROOBr species in both experiments. Previous evidence for the existence of ROOX, where X is a halogen atom, was provided by the work of Jenkin and Cox,[12] who were able to assign transient absorptions in the photolysis of RI–O_2 to ROOI which possessed an unstructured UV absorption spectrum similar to that observed here but with λ_{max} at *ca.* 290 nm. In further experiments[13] in which C_2H_5Br and HOC_2H_4Br were photolysed in the presence of O_2, similar transient absorptions were seen and assigned to C_2H_5OOBr and HOC_2H_4OOBr, both arising from a fast reaction (estimated rate constant *ca.* 10^{-10} cm^3 molecule^{-1} s^{-1} at 760 Torr) between RO_2 and Br. The spectra of C_2H_5OOBr and HOC_2H_4OOBr (λ_{max} at *ca.* 260 nm) appear to be consistent with those of C_2H_5OOBr and BrC_2H_4OOBr measured in the present work.

In studies of the flash excitation of Br_2 with visible radiation, broad, unstructured absorptions near 250 nm were observed.[14,15] These absorptions are thought to be due to excited states of Br_2, which decay over a μs timescale and clearly cannot be identified with the longer-lived transients observed in this work.

Self-reaction Kinetics and Absorption Cross-section at 270 nm

Having identified $BrCH_2CH_2OOBr$ as the transient product in the $BrCH_2CH_2O_2$ experiments it was possible to continue with the kinetic investigations under experimental conditions which reduced its production rate to a minimum. This implies high C_2H_4 and O_2 partial pressures.

As shown in reactions (7*a*) and (9), HO_2 is expected to be produced in secondary chemistry following the self-reaction of $BrCH_2CH_2O_2$. In order to avoid monitoring both $BrCH_2CH_2O_2$ and HO_2 simultaneously, all experiments were carried out with kinetic analysis at 270 nm where the HO_2 radical no longer absorbs.[11] Measurements at this wavelength will also suffer from the least interference from absorption by stable products.

The results from a total of 17 experiments at 400 and 600 Torr are listed in Table 1 together with a further seven experiments at 200 Torr which included low C_2H_4 and O_2 partial pressures. The 12 experiments at 400 Torr give values of $\sigma_{270}(BrCH_2CH_2O_2)$ and k_{7obs} of $(2.19 \pm 0.16) \times 10^{-18}$ cm^2 molecule^{-1} and $(6.07 \pm 0.63) \times 10^{-12}$ cm^3 molecule^{-1} s^{-1}, respectively. As 600 Torr the corresponding results from five experiments are $\sigma_{270}(BrCH_2CH_2O_2) = (2.25 \pm 0.27) \times 10^{-18}$ cm^2 molecule^{-1} and $k_{7obs} = (6.36 \pm 1.03) \times 10^{-12}$ cm^3 molecule^{-1} s^{-1}. As these results are indistinguishable within the error limits, overall values of $\sigma_{270}(BrCH_2CH_2O_2) = (2.20 \pm 0.20) \times 10^{-18}$ cm^2 molecule^{-1} and $k_{7obs} = (6.16 \pm 0.78) \times 10^{-12}$ cm^3 molecule^{-1} s^{-1} are taken from all 17 experiments. The quoted error limits are twice the standard deviation and reflect precision only. k_{obs} and σ data from the 200 Torr experiments were not included in the final analysis as they were expected to be less reliable owing to higher rates of $BrCH_2CH_2OOBr$ formation.

Fig. 4 shows the decay part of a modulated absorption profile due to $BrCH_2CH_2O_2$ at 270 nm and 400 Torr together with the modified second-order fit to the data. As will be discussed later, k_{7obs} the measured self-reaction rate constant, is expected to be greater than k_7 due to the influence of reaction (10).

UV Spectrum

The relative UV spectrum of $BrCH_2CH_2O_2$ was measured at 10 nm intervals between 200 and 280 nm by measuring the steady-state absorbance at each wavelength relative to that at 270 nm obtained under identifical experimental conditions. These experiments were carried out in groups of three with the middle measurements always at 270 nm to ensure that experimental parameters such as k_{phot} or $[Br_2]$ were unchanged.

Absolute cross-sections were obtained by scaling the relative spectrum to $\sigma_{270}(BrCH_2CH_2O_2) = 2.20 \times 10^{-18}$ cm^2 molecule^{-1} and are listed in Table 2 and displayed in Fig. 5. At $\lambda < 260$ nm the presence of HO_2 is likely to result in a composite absorption due to both radicals and may result in an enhanced absorption at these wavelengths (see discussion). At $\lambda \geqslant 270$ nm absorption due to HO_2 is negligible and the absorption is due to $BrCH_2CH_2O_2$ alone. The solid triangles in Fig. 5 represent the individual measurements, the solid lines are from computer fits to the data and are also described in the discussion.

$(CH_3)BrCHCH(CH_3)O_2$

The rate constant for reaction between Br and C_4H_8 is a factor of *ca.* 50 faster than for Br + C_2H_4 and is also dependent on the partial pressure of O_2.[10] By carrying all experiments out with *ca.* 9 Torr C_4H_8 and 240 Torr O_2 in a total pressure of 400 Torr, the reaction between Br and $(CH_3)BrCHCH(CH_3)O_2$ can be avoided. All kinetic data and absolute cross-section measurements were carried out at 270 nm as for $BrCH_2CH_2O_2$ and the relative absorption spectrum was also measured in an identical fashion.

Attempts were made to measure the photolysis constant, k_{phot}, by monitoring the first-order decay of Br_2 (at 500 nm) during the photolysis of static Br_2–C_4H_8–O_2–N_2 mixtures. During these experiments, an unexpected dark decay of Br_2 in C_4H_8 [(1–9) $\times 10^{17}$ molecule cm^{-3}] and *ca.* 400 Torr O_2 was observed, and found to follow approximate first-order kinetics. A rate constant for the reaction between Br_2 and C_4H_8 of 2.7×10^{-21} cm^3 molecule^{-1} s^{-1} was estimated. However the second-order plot revealed a significant non-zero intercept, implying that part of the decay may have been heterogeneous and no conclusions are drawn concerning the

Table 2 The UV absorption spectra of $BrCH_2CH_2O_2$ and $(CH_3)BrCHCH(CH_3)O_2$

	$\sigma/10^{-18}$ cm^2 molecule^{-1}			
	$BrCH_2CH_2O_2$		$(CH_3)BrCHCH(CH_3)O_2$	
λ/nm	M	F	M	F
200	3.50	0.52		
205		0.86		
210	4.33	1.30	2.28	0.94
215		1.83		1.41
220	4.91	2.42	3.39	1.98
225		3.00		2.59
230	4.97	3.50	4.00	3.19
235		3.87		3.71
240	4.88	4.07	4.42	4.10
245		4.06		4.29
250	4.36	3.88	4.29	4.29
255		3.55		4.10
260	3.28	3.12	3.77	3.75
265		2.63		3.30
270	2.20	2.15	2.19	2.80
275		1.69		2.29
280	1.25	1.29	1.80	1.81
285				1.39
290	—		0.84	1.03

M are the measured data, F are the fitted results with deconvolution of HO_2. Cross-sections at uneven wavelengths are extrapolated. Fitted values for $BrCH_2CH_2O_2$ are $\lambda_{max} = 242.4$ nm; $\sigma_{max} = 4.09 \times 10^{-18}$ cm^2 molecule^{-1} and $a = 55.6$, and for $(CH_3)BrCHCH(CH_3)O_2$ $\lambda_{max} = 247.4$ nm; $\sigma_{max} = 4.31 \times 10^{-18}$ cm^2 molecule^{-1} and $a = 56.7$.

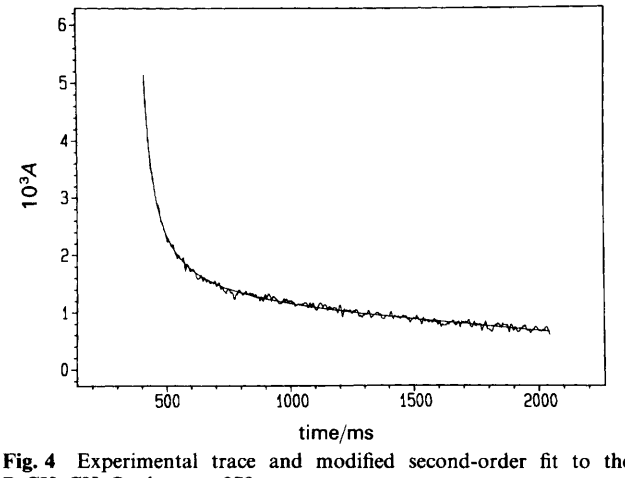

Fig. 4 Experimental trace and modified second-order fit to the $BrCH_2CH_2O_2$ decay at 270 nm

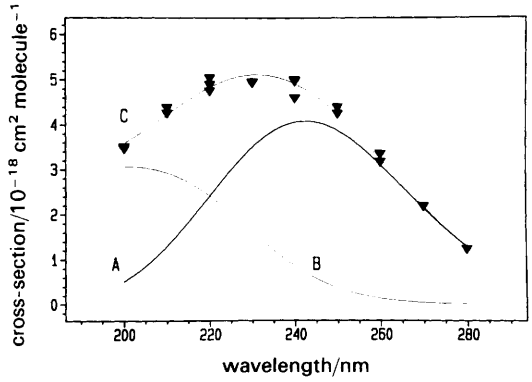

Fig. 5 UV absorption spectra of $BrCH_2CH_2O_2$. Solid triangles are experimentally determined points. A and B are the deconvoluted spectra of $BrCH_2CH_2O_2$ and HO_2, respectively, C is the composite absorption

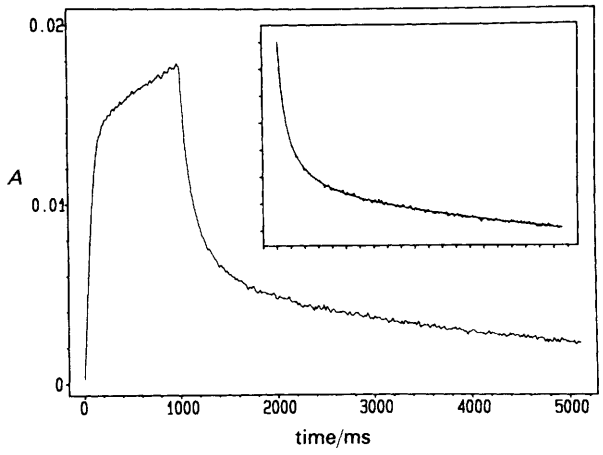

Fig. 6 Modulated absorption profiles at 270 nm due to $(CH_3)BrCHCH(CH_3)O_2$ in the Br_2–C_4H_8–O_2–N_2 system. $[Br_2]_0 = 1.56 \times 10^{15}$ molecule cm^{-3}, $O_2 = 236$ Torr, $C_4H_8 = 9$ Torr, $P_{total} = 400$ Torr. The inset shows the modified second-order fit to the decay during the lights-off period

mechanism or possible products of this reaction. Given the concentrations of C_4H_8 in a typical photolysis experiment (*ca.* 3×10^{17} C_4H_8), the first-order loss of Br_2 due to the reaction with C_4H_8 will be *ca.* 6×10^{-4} s^{-1} and therefore negligible compared to its removal rate by photolysis (1.5×10^{-2} s^{-1}).

Self-reaction Kinetics and Absorption Cross-section at 270 nm

All experiments were carried out in flowing mixtures of *ca.* 1.5×10^{15} molecule cm^{-3} Br_2, 9 Torr of C_4H_8, 236 Torr of O_2 and N_2 added to give a total pressure of 400 Torr. A typical modulated absorption profile at 270 nm is shown in Fig. 6, the inset shows the modified second-order fit to the decay. The results for eight experiments were evaluated to give the values of $\sigma_{270}(CH_3BrCHCHCH_3O_2)$ and k_{8obs} listed in Table 3. The final results are $\sigma_{270}(CH_3BrCHCHCH_3O_2) = (2.91 \pm 0.29) \times 10^{-18}$ cm^2 molecule^{-1}, and $k_{8obs} = (9.56 \pm 1.37) \times 10^{-13}$ cm^3 molecule^{-1} s^{-1}. In both cases the quoted errors are twice the standard deviation, reflecting precision only.

Analagous to $BrCH_2CH_2O_2$, the self-reaction of $(CH_3)BrCHCH(CH_3)O_2$ is expected to proceed *via* at least two channels:

$$2\ (CH_3BrCHCH(CH_3)O_2 \rightarrow 2\ (CH_3)BrCHCH(CH_3)O + O_2 \quad (8a)$$

$$\rightarrow (CH_3)BrCHCH(CH_3)OH + (CH_3)BrCHC(O)CH_3 + O_2 \quad (8b)$$

The $(CH_3)BrCHCH(CH_3)O$ radical generated in reaction (8*a*) will react with O_2 to give HO_2 (18) which can react with

Table 3 Kinetic and UV cross-section data for $(CH_3)BrCHCH(CH_3)O_2$ at 270 nm

expt.	σ_{270} /10^{-18} cm^2 molecule^{-1}	k_{8obs} /10^{-13} cm^3 molecule^{-1} s^{-1}
1	2.75	8.66
2	2.94	9.88
3	3.05	10.1
4	2.84	9.18
5	3.06	10.3
6	3.10	10.2
7	2.85	9.59
8	2.72	8.56

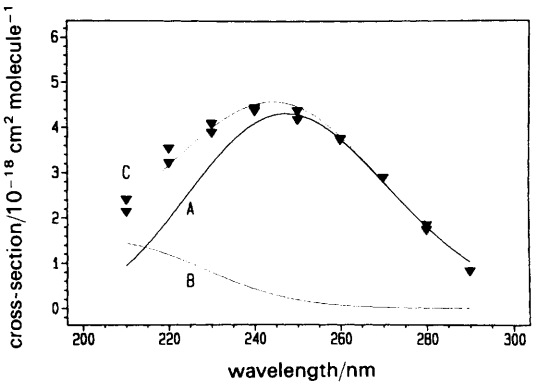

Fig. 7 UV absorption spectra of $(CH_3)BrCHCH(CH_3)O_2$. Solid triangles are experimentally determined points. A and B are the deconvoluted spectra of $BrCH_2CH_2O_2$ and HO_2, respectively, C is the composite absorption

$(CH_3)BrCHCH(CH_3)O_2$ (19) or with itself (11).

$$(CH_3)BrCHCH(CH_3)O + O_2 \rightarrow (CH_3)BrCHC(O)CH_3 + HO_2 \quad (18)$$

$$(CH_3)BrCHCH(CH_3)O_2 + HO_2 \rightarrow (CH_3)BrCHCH(CH_3)OOH + O_2 \quad (19)$$

UV Absorption Spectrum

The relative absorption spectrum of $(CH_3)BrCHCH(CH_3)O_2$ was measured between 210 and 290 nm as for $BrCH_2CH_2O_2$ and scaled to the absolute value of 2.91×10^{-18} cm^2 molecule^{-1} at 270 nm. The cross-sections are listed in Table 2 and the measured data (solid triangles) are depicted at 10 nm intervals in Fig. 7. The solid lines are fitted curves and are described below.

Discussion

In general, alkylperoxy radical self-reactions may proceed *via* at least two channels, leading to stable products or to alkoxy radicals. In the presence of O_2, the rate of smaller alkoxy radicals, including ethyl-[1] and 1-methylpropyl[16] is reaction to generate HO_2:

$$2\ RO_2 \rightarrow 2\ RO + O_2 \quad (ia)$$

$$\rightarrow ROH + R'HO \quad (ib)$$

$$RO + O_2 \rightarrow HO_2 + R'HO \quad (ii)$$

$$RO_2 + HO_2 \rightarrow ROOH + O_2 \quad (iii)$$

A consequence of the secondary production of HO_2 and subsequent reaction (iii) is that the observed decay rate of RO_2 will be enhanced over the true self-reaction rate. For this reason we have adopted the term k_{iobs} to refer to the experimental rate constant. As discussed by Lightfoot *et al.*,[1] the fraction by which k_{iobs} is greater than k_i depends on the rate of reactions (i) and (iii) and the value (k_{ia}/k_{ib}).

For $BrCH_2CH_2O_2$ self-reaction, the ratio (k_{ia}/k_{ib}) has been measured recently as 1.35.[9] If we assume that the rate constant for reaction between HO_2 and $BrCH_2CH_2O_2$ is similar to that between HO_2 and $C_2H_5O_2$ (5.8×10^{-12} cm^3 molecule^{-1} s^{-1}),[1] we can estimate that *ca.* 45% of HO_2 radicals generated *via* reactions (7*a*) and (9) will react with $BrCH_2CH_2O_2$ during the radical decay period, resulting in an overall enhancement in the rate constant for self reaction (k_7) of *ca.* 25%.

For $(CH_3)BrCHCH(CH_3)O_2$, as neither (k_{ia}/k_{ib}) nor k_{iii} are known, we can only present data for k_{iobs}. However, as k_{iobs} (or k_{iobs}/σ) is the measured parameter in all peroxy radical

self-reaction studies,[1] direct comparisons can be made with values of k_{iobs} for other RO_2 species.

The presence of HO_2 in sufficiently high concentrations will also alter the shape of the UV absorption spectrum of RO_2 where the two spectra overlap. Numerical simulations showed that, for RO_2 self-reactions with $k_{obs} > 5 \times 10^{-13}$ cm^3 $molecule^{-1}$ s^{-1} and a significant branching ratio to RO, HO_2 concentrations similar to RO_2 may be present during the radical steady-state period.

The result of such a simulation is shown in Fig. 8 which displays modulated absorption profiles from a peroxy radical undergoing self-reaction (curve A) to generate both HO_2 (curve B) and a product (curve C). As described above, the ratio of RO_2 to HO_2 depends on several constants. In this case a value k_7 of 4×10^{-12} cm^3 $molecule^{-1}$ s^{-1} was used with a 50% branching ratio into the (*ia*) and (*ib*) channels. RO was converted instantaneously to HO_2 and a rate constant of 6×10^{-12} cm^3 $molecule^{-1}$ s^{-1} was chosen for the $HO_2 + RO_2$ reaction. The rate constant for HO_2 self-reaction used was 2.5×10^{-12} cm^3 $molecule^{-1}$ s^{-1}. The results show that HO_2 reaches a steady-state concentration *ca.* 40% that of RO_2. RO_2 spectra measured under such steady-state conditions will therefore suffer from HO_2 interference at shorter wavelengths and must be corrected. The correction (deconvolution) procedure adopted is outlined below.

Error Analysis

Of fundamental importance to the kinetic analysis performed in these experiments is the accurate measurement of the Br_2 photolysis constant, k_{phot}, and the Br_2 concentration, which together determine the production rate of R and thus RO_2. k_{phot} was measured frequently and showed little fluctuation about its two values (see text). The combined error in $[Br_2]$ measurement (and its correction) and k_{phot} is thought not to exceed 5%. The assumption is also made that all Br atoms lead to RO_2 formation, clearly this is not the case if large amounts of $BrCH_2CH_2OOBr$ are produced. Examination of the modulated profile at 600 Torr in Fig. 1 reveals a *ca.* 15% contribution to absorption at the end of the photolysis period by the stable absorber. Assuming that this is due to $BrCH_2CH_2OOBr$ only, and that RO_2 and ROOBr have similarly intense absorption spectra, then, because ROOBr absorbs *ca.* twice as strongly at 270 nm as does RO_2, ROOBr will be present at *ca.* 7% of RO_2. Also to be considered is that end products also absorb at 270 nm, and we estimate that $<5\%$ of Br can react with RO_2 in our experiments. This conclusion is borne out by the fact that experiments with differing rates of $BrCH_2CH_2OOBr$ production (400 and 600 Torr) give the same values for σ_{270}, as indeed do the 200 Torr experiments where $BrCH_2CH_2OOBr$ production was most pronounced. The reaction between Br and $BrCH_2CHO$ is too slow to represent a potential loss of Br atoms in the present experiments.[9] In the light of this an additonal error of $<5\%$ may be estimated.

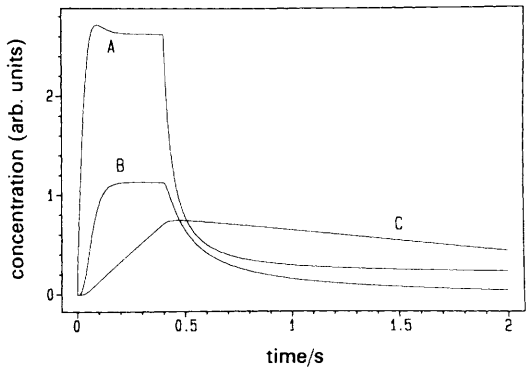

Fig. 8 Modulted concentration profiles from numerical simulations of a $BrCH_2CH_2O_2$ experiment. A, a peroxy radical undergoing self-reaction (second-order behaviour). B, HO_2 profiles, where HO_2 is a product of secondary chemistry. C, the aldehydic product of the radical self-reaction in a flowing system. Measured experimental values of k_{phot}, $[Br_2]$ and k_f (flow rate) were used in these simulations

In the modified second-order analysis, the decay part of the absorption profile is fitted to an algorithm that contains a term which varies linearly. This is to take care of absorption by a product that does not follow second-order kinetics but is lost by flow out of the cell. Examination of the product profile (curve C) in Fig. 8 reveals a triangular function confirming that the modified second-order analysis is adequate under our flow conditions.

In the light of these considerations we increase our error limits on k_{obs} to $\pm 20\%$ to include both experimental scatter and possible systematic error.

Deconvolution of Composite Absorption Spectra

As suggested in the text, the presence of HO_2 may result in composite absorptions at $\lambda < 270$ nm in the $(CH_3)BrCHCH(CH_3)O_2$ and especially in the $BrCH_2CH_2O_2$ experiments. It has recently been shown,[1,17] that a Gaussian distribution function of the form

$$\sigma(T) = \sigma_{max}(T)\exp\{-a(T)[\ln(\lambda_{max}/\lambda)]^2\} \quad (v)$$

accurately reproduces the shapes of peroxy radical spectra, and in a modified form may be used to deconvolute composite absorptions. In this equation, σ_{max} and λ_{max} have their usual meanings, T is the temperature, and a is a term which defines the width of the absorption spectrum. We make the assumption here that $BrCH_2CH_2O_2$ and $(CH_3)BrCHCH(CH_3)O_2$ spectra are also described by equation (v).

When the measured UV spectra of both $BrCH_2CH_2O_2$ and $(CH_3)BrCHCH(CH_3)O_2$ are fitted to an algorithm which represents two absorption bands, the best fit is obtained when an additional absorber with a maximum between 200 and 210 nm is present. This is clearly due to HO_2 which, as described in the text, is expected to be present in significant concentrations. The measured composite UV spectra of both $BrCH_2CH_2O_2$–HO_2 and $(CH_3)BrCHCH(CH_3)O_2$–HO_2 were therefore fitted to a double Gaussian function in which one of the absorptions was identical in shape to the UV spectrum of HO_2.[1] This procedure enables the true RO_2 UV absorption to be deconvoluted from the composite absorption, and results in the solid curves in Fig. 5 and 7. In each case three curves are displayed which represent A, the RO_2 contribution, B, the HO_2 contribution and C, the composite absorption through the measured points. The true UV spectra of $BrCH_2CH_2O_2$ and $(CH_3)BrCHCH(CH_3)O_2$ can now be described by the three parameters λ_{max}, σ_{max} and a which are listed in Table 2. Parametrisation of the spectra enable accurate extrapolation between measured values and cross-sections at 5 nm intervals taken from the fit and these values are listed in Table 2. The complete spectrum may be generated at any required wavelength interval using eqn. (v). The accuracy of the deconvolution process depends to a large extent on the quality of the fitted data, especially at shorter wavelengths where the HO_2 contribution to the absorption is greatest. In cases where only a few points have been measured (*i.e.* this work) errors of 20% in the amount of HO_2 subtracted cannot be ruled out.

Comparison with Other Peroxy Radical Spectra and Kinetics

In this section we compare the UV spectra and self-reaction kinetics of $BrCH_2CH_2O_2$ and $(CH_3)BrCHCH(CH_3)O_2$ with each other and with other peroxy radicals. For this purpose, we consider $(CH_3)BrCHCH(CH_3)O_2$ to be a dimethyl substituted form of the ethylperoxy radical.

Self-reaction Kinetics at 298 K

The greater self-reaction rate constant at $BrCH_2CH_2O_2$ (6.16×10^{-12} cm^3 $molecule^{-1}$ s^{-1}) as compared to unsubstituted $C_2H_5O_2$ (1.1×10^{-13} cm^3 $molecule^{-1}$ s^{-1}),[4] tends to confirm the trend seen for $ClCH_2CH_2O_2$, $ClCF_2CH_2O$ and $FCCl_2CH_2O_2$ that halogen substitution at the β position in $C_2H_5O_2$ has a significant enhancement effect on the rate constant.[1] A factor *ca.* 60 is observed for β-bromination, whereas the effect of β-fluorination/chlorination is to enhance the rate constant by a factor of *ca.* 30–40. Note also that a recent measurement of the $BrCH_2O_2$ self-reaction rate constant, $k_{obs}(BrCH_2O_2)$, of 3.26×10^{-11} cm^3 $molecule^{-1}$ s^{-1},[3] is a factor of *ca.* 60 greater than $k_{obs}(CH_3O_2)$ (4.8×10^{-13} cm^3 $molecule^{-1}$ s^{-1}) at 298 K,[1] and a factor of 10 or more greater than the measured value of k_{obs} for the chlorinated and fluorinated counterparts of CH_3O_2,[1] in accordance with the trends seen here for $BrCH_2CH_2O_2$. For the purpose of comparison, $(CH_3)BrCHCH(CH_3)O_2$ may be seen as an α,β methyl-substituted form of $BrCH_2CH_2O_2$. The result of methylation is to decrease the self-reaction rate constant of the resulting secondary peroxy radical $(CH_3)BrCHCH(CH_3)O_2$ by a factor of *ca.* 6.

UV Absorption Spectra

For the purpose of comparing UV spectra of $BrCH_2CH_2O_2$ and $(CH_3)BrCHCH(CH_3)O_2$ we use the deconvoluted spectra as listed in Table 2. It is apparent that all three spectra are very similar, with absorption maxima between 240 and 250 nm and in all cases a σ_{max} close to 4×10^{-18} cm^2 $molecule^{-1}$. This indicates little interaction between the β Br atom and the chromophore responsible for the electronic transition (n–π^*) which is known to reside largely on the O—O part of the molecule.

Summary

The self-reaction rate constant (k_{obs}) for 2-bromoethylperoxy radicals ($BrCH_2CH_2O_2$) at 298 K is considerably larger than for the unsubstituted ethylperoxy radical ($C_2H_5O_2$). This confirms the trend seen for other peroxy radicals in which halogenation, and especially bromination, significantly enhances k_{obs}. Dimethylation of $BrCH_2CH_2O_2$ to give 2-bromo-1-methylpropylperoxy radicals, $(CH_3)BrCHCH(CH_3)O_2$, results in a reduction in k_{obs}. The UV spectra of $BrCH_2CH_2O_2$ and $(CH_3)BrCHCH(CH_3)O_2$ reveal little deviation from that of $C_2H_5O_2$.

We would like to thank D. Maric for some assistance in carrying out the deconvolution fits. This work was carried out with financial support from the CEC (projects STEP and LACTOZ).

References

1 P. D. Lightfoot, R. A. Cox, J. N. Crowley, M. Destriau, G. D. Hayman, M. E. Jenkin, G. K. Moortgat and F. Zabel, *Atmos. Environ. A*, 1992, **26**, 1805.
2 P. Dagaut, T. J., Wallington and M. J. Kurylo, *Chem. Phys. Lett.*, 1988, **146**, 589.
3 O. J. Nielsen, J. Munk, G. Locke and T. J. Wallington, *J. Phys. Chem.*, 1991, **95**, 8714.
4 D. Bauer, J. N. Crowley and G. K. Moortgat, *J. Photochem. Photobiol. A: Chem.*, 1992, **65**, 329.
5 H. Okabe, *Photochemistry of Small Molecules*, Wiley, New York, 1978.
6 R. J. Donovan and D. Husain, *Trans. Faraday Soc.*, 1966, **62**, 2987.
7 M. E. Jenkin and R. A. Cox, *J. Phys. Chem.*, 1985, **89**, 192.
8 R. A. Cox and J. P. Burrows, *J. Phys. Chem.*, 1979, **83**, 2560.
9 G. Yarwood, N. Peng and H. Niki, *Int. J. Chem. Kinet.*, 1992, **24**, 369.
10 I. Barnes, V. Bastian, K. H. Becker, R. Overath and Zhu Tong, *Int. J. Chem. Kinet.*, 1989, **21**, 499.
11 J. N. Crowley, F-G. Simon, J. P. Burrows, G. K. Moortgat, M. E. Jenkin and R. A. Cox, *J. Photochem. Photobiol. A: Chem.*, 1991, **60**, 1.
12 M. E. Jenkin and R. A. Cox, *J. Phys. Chem.*, 1991, **95**, 3229.
13 G. D. Hayman, M. E. Jenkin and T. P. Murrells, *Eurotrac Annual Report*, Commission of the European Communities, Garmisch-Partenkirchen, 1990, Part 8.
14 S. L. Shostak and R. L. Strong, *Chem. Phys. Lett.*, 1979, **63**, 370.
15 L. H. MacDonald and R. L. Strong, *J. Phys. Chem.*, 1991, **95**, 6940.
16 A. Heiss, J. Tardieu de Maleissye, V. Viossat, K. A. Sahetchian and I. G. Pitt, *Int. J. Chem. Kinet.*, 1991, **23**, 607.
17 J. N. Crowley, D. Maric and J. P. Burrows, in preparation.

Paper 2/01129H; *Received* 3rd *March*, 1992